Opt Quant Electron (2016) 48:160
DOI 10.1007/s11082-015-0287-y

Ab initio study on the structural, electronic, optical and electrical properties of Mo-, Nb- and Ta-doped rutile SnO_2

Amine Slassi[1]

Received: 5 March 2015 / Accepted: 8 September 2015 / Published online: 2 February 2016

Abstract We show the effect of molybdenum-, niobium- and tantalum-dopants on the structural, electronic, optical and electrical of tin dioxide by using first-principle study within the full-potential linearized augmented plane wave method and semiclassical Boltzmann transport theory. The results show that the doped tin dioxide systems have negative formation energies. The dopants introduce shallow donor states around the conduction band minimum, leading to red-shift of optical transparency in the case of molybdenum- and niobium-doped tin dioxide, and blue-shift in the case of tantalum doped tin dioxide. The electrical conductivity is remarkably improved after doping, while the tantalum doped tin oxide exhibits the highest value.

Keywords Tin dioxide · Ab initio · Semiclassical Boltzmann theory · Transparent conducting oxide

1 Introduction

Tin dioxide SnO_2 is a wide band gap semiconductor with an ideal direct band gap of 3.6 eV. Advantages, such as low cost, non-toxicity and high thermodynamic stability, make it widely requested in many optoelectronic applications including transparent conducting electrode, light emitting diodes and photocatalyst (Yates et al. 2012; Ouerfelli et al. 2008; Park et al. 2015). In order to improve the efficiently of SnO_2 in technological applications, many attempts on doping of SnO_2 have been investigated (Orel et al. 1995; Turgut et al. 2013; Toyosaki et al. 2008). Mo, Nb and Ta are the most interesting doped elements into SnO_2 structure to decrease the electrical resistivity due to difference of oxidation number between native and these dopant elements. For example, Ta-doped SnO_2

✉ Amine Slassi
a.slassi@yahoo.fr; a.slassi22@gmail.com

[1] LMPHE (URAC 12), Faculté des Sciences, Université Mohammed V-Agdal, Rabat, Morocco

were reported to exhibit a low resistivity of 1.1×10^{-4} Ω cm (Toyosaki et al. 2008), which is comparable that of F-doped SnO_2. More recently, the attempts have been done to find other dopant elements for improving the efficiency of SnO_2 properties, such as Mo and Nb (Orel et al. 1995; Turgut et al. 2013). Nevertheless, the electrical resistivity of Nb-doped SnO_2 was reported to be 0.62×10^{-3} Ω cm (Turgut et al. 2013), while that of Mo-doped SnO_2 was 1.7×10^{3} Ω cm (Orel et al. 1995). Despite, there aren't enough studies on the structural, electronic, optical and electrical properties of Mo-, Nb- and Ta-doped SnO_2.

The theoretical methods such as density functional theory (DFT) provide an extremely valuable tool for predicting different properties of a large number of semiconductors (Slassi 2015; Zhang et al. 2012; Shi et al. 2013; Qin et al. 2009; Dixit et al. 2012; Slassi et al. 2014; Tran and Blaha 2009). Interestingly, first-principles-based calculation can serve as a predictive tool to development of new materials. However, the main limitation of first principles study is the ability to produce the band gap of semiconductors in good agreement with that of experimental measurement due to exchange–correlation terms. A theoretical point of view, the standard DFT calculations yield band gap values much underestimate as compared to experimental data. The band gap of rutile SnO_2 was reported to be 1.2 eV by using the generalized gradient approximation (Zhang et al. 2012), and 1.307 eV by the local density approximation (Shi et al. 2013). Some moderate methods have recently been developed to correct band gap error such as Tran–Blaha modified Becke–Johnson (TB-mBJ) (Tran and Blaha 2009). This yield a band gap value less underestimated to experimental data.

2 Theoretical and computational approaches

In the present first principle study, we have employed the full potential linearized augmented plane wave (FP-LAPW) method to solve the Kohn–Sham equations as implemented in the Wien2k code (Blaha et al. 2001; Georg 2001). The exchange–correlation potential was described within the generalized gradient approximation (GGA-PBE) proposed by Perdew et al. (1996) to investigate the structural properties, while Tb-mBJ for electronic, optical and electrical properties. The radii of the muffin tin atomic spheres R_{MT} are 2.03 Bohr for Sn, Mo, Nb and Ta atoms, and 1.75 Bohr for O, respectively. The cutoff parameter R_{MT} K_{MAX} is set to 7.0 where R_{MT} denotes the smallest muffin tin radius of atoms and K_{MAX} is the maximum value of the reciprocal lattice vectors used in the plane wave expansion. We have used a self-consistent criterion of the total energy with a precision of 0.0001 Ry.

3 Discussion of results

3.1 Structural properties

Tin dioxide SnO_2 crystallizes in rutile tetragonal structure in the nature state with a space group I41/AMD, containing two Sn- and four O-atoms in the primitive unit cell (Kim et al. 1994). A $2 \times 2 \times 2$ supercell consisting of 42 was constructed in the calculations. To simulate the effect of doping on SnO_2 properties, we substituted a Sn atom by a Mo, Nb or Ta atom in 42 atoms supercell, as shown in Fig. 1, that corresponds to level doping of

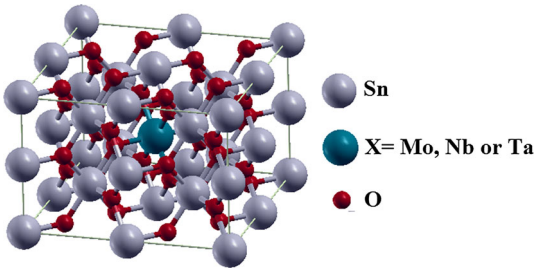

Fig. 1 2 × 2 × 2 Supercell model of doped rutile-SnO_2

6.5 %. The equilibrium lattice constants and energy of ground states are evaluated by fitting the energy versus volume data into the Murnaghan equation of state (Murnaghan 1944).

The optimized lattice constants of pure and doped SnO_2 systems are summarized in Table 1. The current calculated lattice constants of pure SnO_2 are in good agreement with other theoretical results and slightly bigger than the experimental values due to the well-known overestimation of GGA, indicating that our results are still reliable. For doping cases, the constant lattices of Mo-doped SnO_2 system decrease from pure, while ones of Ta- and Nb-doped SnO_2 expand owing to the difference in the atomic radii between native and dopant elements.

To check the thermodynamic stability of doped systems, the formation energies (Bai et al. 2011) for Mo, Nb- and Ta-doped SnO_2 have been estimated:

$$\begin{aligned} E_{form}(\text{X-doped } SnO_2) = {} & E(\text{X-doped } SnO_2) - E(\text{pure}) - E(X) \\ & + E(Sn)(X = \text{Mo, Nb and Ta}) \end{aligned}$$

where E(X-doped SnO_2), E(pure) are the total energy of pure and doped supercell systems, respectively; E(Sn) and E(X) represent the total energy per atom of Sn and X=Mo, Nb and Ta bulk. The more stable system has the lower energy. The different values of formation energies are summarized in Table 1. It can be seen from values that the doped systems have negative formation energy, demonstrating that the doped SnO_2 system becomes more stable after doping with Mo-, Nb- or Ta-atoms. This give the opportunity to make experimentally doped SnO_2 samples with the minimum of structural defects. In addition, the Ta-doped SnO_2 shows the lower formation energy, giving the advantage to the Ta-dopant. Singh et al. (2008) reported that the doping with Nb- and Ta-elements on Sn native

Table 1 Calculated lattice constants and formation energies of pure and doped rutile-SnO_2 by using GGA-PBE

System	a (A°)	c (A°)	E_f/eV
Pure SnO_2	4.8304	3.2465	
Exp.	4.747 (Kim et al. 1994)	3.186 (Kim et al. 1994)	
DFT-GGA	4.825 (Hassan et al. 2005)	3.245 (Hassan et al. 2005)	
	4.821 (Duan 2008)	3.236 (Duan 2008)	
Mo-doped SnO_2	4.8290	3.2455	−0.887
Nb-doped SnO_2	4.8361	3.2504	−3.741
Ta-doped SnO_2	4.8373	3.2512	−4.162

atom site lead to negative formation energies, which is in good agreement with our calculations.

3.2 Electronic structure

To better understand the impact of doping on the electronic structure of SnO_2 system; the band structure and projected density of states are examined. The band structure of pure-, Mo-, Nb and Ta-doped SnO_2 along the Z–A–X–G–Z–R–X–G path in the first Brillouin zone are shown in Fig. 2. It's clear from Fig. 2a that the valence band maximum and the conduction band minimum locate at the same G-point, indicating that the lowest band gap transition in the SnO_2 rutile is direct, which is in conformity with the previous theoretical calculations (Zhang et al. 2012; Shi et al. 2013; Qin et al. 2009; Dixit et al. 2012). The calculated band gap value for pure SnO_2, using Tb-mBJ approach, is about 2.63 eV, which is underestimated as compared to experimental values due to the well-known drawback of DFT based calculations. Nevertheless, this result presents a lower underestimation of band gap than the GGA calculation that gives only 1.2 eV. On the other hand, the electrical behaviour was substantially evaluated from the energy dispersion at the top of the valence

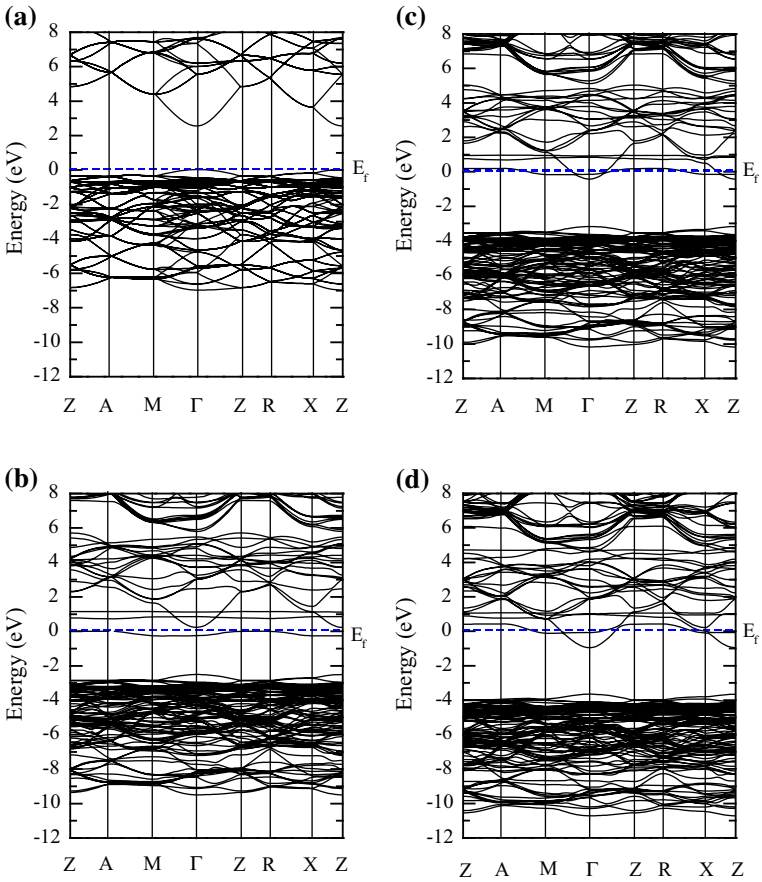

Fig. 2 Band structure of: **a** pure, **b** Mo-, **c** Nb- and Ta-doped rutile-SnO_2 using TB-mBJ, respectively

Table 2 Calculated optical band gaps of pure and doped rutile-SnO_2 by using TB-mBJ

System	E_g (eV)
Pure SnO_2	2.63
Mo-doped SnO_2	2.46
Nb-doped SnO_2	2.51
Ta-doped SnO_2	3.68

band and the bottom of the conduction band. The curvature of the conduction band at the G-point, as shown in Fig. 2a, is less flat than that at the top of the valence band, suggesting a lower effective mass of the electron that of the hole in the SnO_2 host. In term of the relation between the electrical conductivity and the absolute value of the effective mass of the free charge carriers, the conductivity of n-type doped SnO_2 is more favourable than that of p-type doped SnO_2 for conducting electrode application.

When Mo-, Nb- or Ta- doped SnO_2, as shown in Fig. 2b–d, the main effects in the band structures are to create donor states and shifting the Fermi level towards the conduction band minimum. These make the doped SnO_2 systems n-type conducting semiconductor. In addition, the Fermi level enters into the conduction band in the case of the Ta-doped SnO_2 make it a degenerate semiconductor; therefore, the Burstein–Moss effect can be predicted. This implies that the optical band gap (from the top of the valence band to the Fermi level) could significantly expand in the Ta-doped SnO_2 system. The different optical band gap values of pure and doped SnO_2 systems are summarized in Table 2. From the results, it is clear seen that the band gap of Mo- and Nb-doped SnO_2 decrease due to occupied states below the conduction band minimum, which affect negatively on the optical transparency. Whereas, the optical band gap for Ta-doped SnO_2 is significantly increased due to, as mentioned above, the Burstein–Moss effect, which is useful for transparent conducting applications.

The total and partial density of states of pure-, Mo-, Nb-, and Ta-doped SnO_2 are presented in the Fig. 3a–d. The Fig. 3a shows that the upper portion of the valence band, for pure SnO_2, mainly derive from the O-2p states with the low contribution of Sn-5p states. The strong contribution of O-2p states, in the top of the valence band, is one of the reasons of the low p-type conductivity in the oxide semiconductors. The bottom portion of the conduction band, in the range -7.6 and 0 eV, consists essentially of Sn-5s and Sn-5p states while O-2s states also have a little presence.

The effect of doping on the electronic properties can be examined from 3b–d. The states created around the Fermi level can govern the major physical properties in the doped SnO_2 system. The case for Mo-doping, as shown in Fig. 3b, the shallow states that occupy a limited range of energy around the Fermi level are formed by the Mo-4d impurity. These impurity states around the Fermi level, as shown in Fig. 3c–d, become shallower for Nb and Ta-doping, indicating that the impurity maybe has a substantial impact on the opto-electronic properties of the doped SnO_2 systems. Furthermore, these shallow states are dominated by Nb-4d and Ta-4d states for Nb- and Ta-doping, respectively. In the electrical behaviour point of view, these impurity states could be considered as the primary origin of the electrical conductivity in the doped SnO_2 systems.

3.3 Optical properties

The optical properties of a material are usually determined by the complex dielectric function $\varepsilon(\omega) = \varepsilon_1(\omega) + i\varepsilon_2(\omega)$, which present the linear response of a system to electromagnetic field. The imaginary part of the dielectric function, $\varepsilon_2(\omega)$, represents the

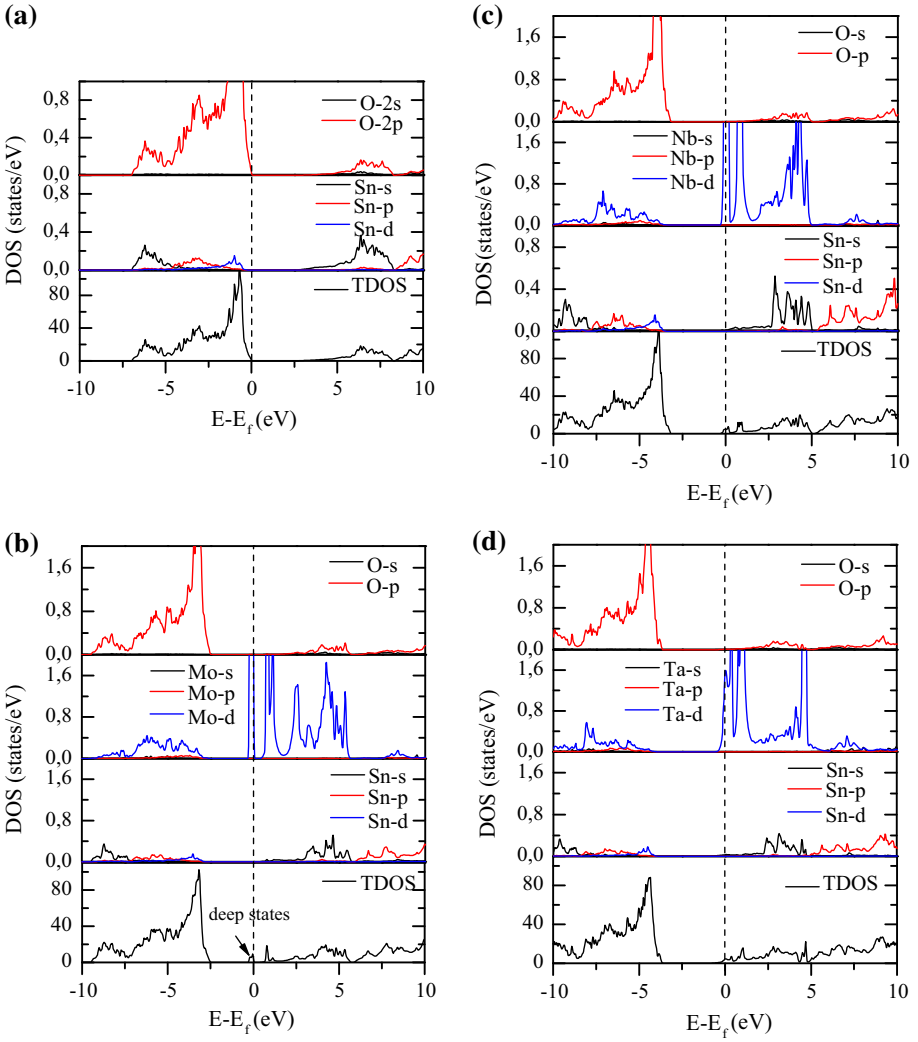

Fig. 3 Total and partial density of states of: **a** pure, **b** Mo-, **c** Nb- and Ta-doped rutile-SnO_2 using TB-mBJ, respectively

absorption in the crystal, which can be obtained by calculating the momentum matrix elements between the occupied and the unoccupied electronic (Okoye 2003). Then, the real part of the dielectric function, $\varepsilon_1(\omega)$, governs the propagation behaviour of electromagnetic field in a material, is derived from the imaginary part using the Kramers–Kronig transformation (Amin et al. 2011). Hence, the linear optical properties, such as the optical reflectivity and the absorption coefficient, could be derived directly from the complex dielectric function (Sun et al. 2005).

The imaginary part of the dielectric function of pure-, Mo-, Nb- and Ta-doped SnO_2 are shown in Fig. 4. The peak, E_1, at energy of about 2.67 eV represents the transition energy threshold, which corresponds to the band gap of pure SnO_2. This threshold shifts to the

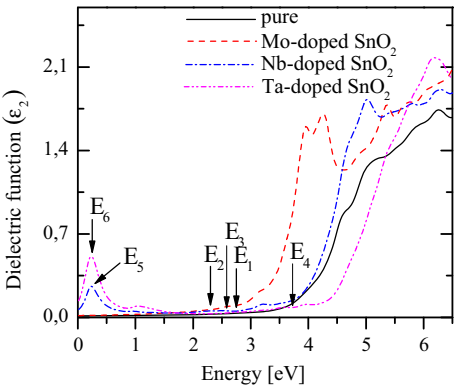

Fig. 4 Imaginary part of dielectric function of pure, Mo-, Nb- and Ta-doped rutile-SnO_2 by using TB-mBJ

lower energy of about 2.46, E_2, eV and 2.51 eV, E_3, in the case of the Mo- and Nb-doped SnO_2 systems, respectively. The reason behind these red shifting is explained by decreasing of band gaps. The pick, E_4, at energy 3.65 eV in the case of Ta-doped SnO_2 is due to, according to the Burstein–Moss effect, the vertical transition between states at the appropriate k-point matching the initial valence band states to the unoccupied states around the Fermi level. Moreover, the picks, E_5 and E_6, at the energies of 0.23 and 0.5 eV represent the electron transition between occupied and unoccupied states localized just around the Fermi level. These low energies of the electron transition suggest that the electron injection into the conduction band could be started from the low excitation energy in the Nb- and Ta-doped SnO_2 samples, which is useful for transparent electrode applications.

The optical transmittance, absorption and reflectivity of pure, Mo-, Nb- and Ta-doped SnO_2 are shown in Fig. 5. A large wavelength transmittance in the visible and UV ranges is required for transparent conducting application. It's clearly, as shown in Fig. 5a, that the pure SnO_2 has an excellent optical transparency along the visible range with an average of 83 %, which is in good agreement with experimental data on the SnO_2 ritule thin films (Gao et al. 2014; Singh and Kumara 2015). The reflectivity for pure SnO_2, as shown in Fig. 5b, is within the average minimum extent of 10 %, while the absorption coefficient, as shown in Fig. 5c, is still low in the visible range due to its semiconducting nature. For doped SnO_2 systems, the average transmittances in the visible region are decreased owing to the induced absorption of shallow states and the reflectivity of area. On the other hand, the threshold of the transmittance is red-shifted for Mo- and Nb-doped SnO_2 systems, while is blue-shifted and the optical transparency is improved towards of UV range that is useful for transparent conducting applications. These blue-shifts are mainly attributed to increasing of the band gap of doped SnO_2 systems. On the experimental point of view, our obtained results are in good agreement with optical data on thin films (Gao et al. 2014; Singh and Kumara 2015).

3.4 Electrical

The reduced electrical conductivity of materials could easily obtained by using the Boltztrap package. This package is based on the semi-classical Boltzmann theory and the rigid band approach (Scheidemantel et al. 2003; Madsena and Singh 2006). However, the main issue in the semi-classical Boltzmann theory is the determination the relaxation time, τ^{-1}, for calculating the exact electrical conductivity. To advance in the calculations, we

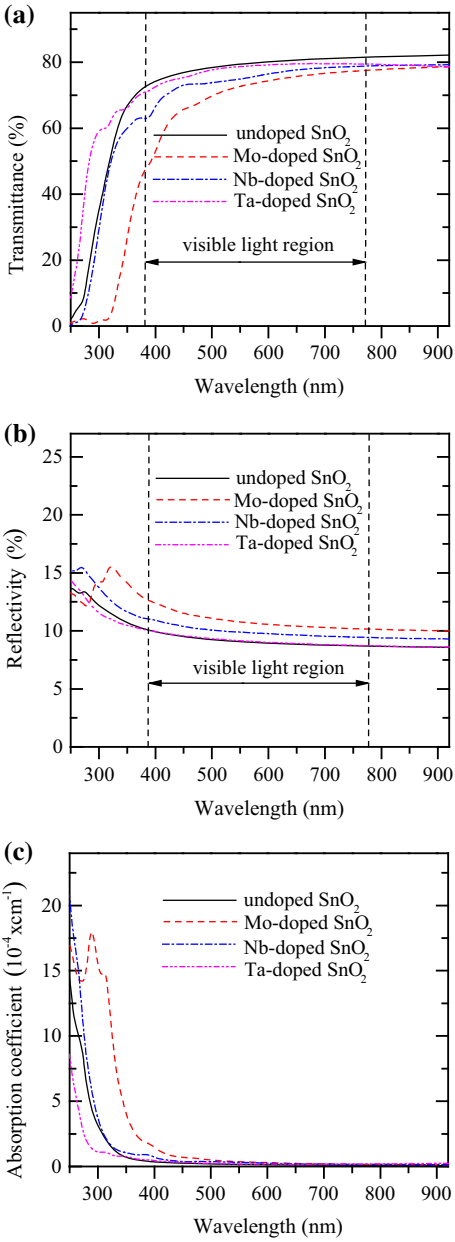

Fig. 5 **a** Transmittance, **b** reflectivity and **c** absorption coefficient of pure and doped rutile-SnO_2, by using TB-mBJ, respectively

used the module proposed by Ong et al. (2011) and experimental data reported by Tsubota et al. (2014), who made measurements on the SnO_2 ceramic. By combining those with our calculations, we obtained the relaxation time, $\tau = 9.98 \times 10^{-6} \times T^{-1} \times n^{-1/3}$. The calculated electrical conductivity for pure-, Mo-, Nb-, Ta-doped SnO_2 are summarized in Table 3. It is clear that the electrical conductivities for doped SnO_2 systems are remarkably improved as compared to that of pure SnO_2. These are due to the difference in the

Table 3 Calculated electrical conductivities of pure and doped rutile-SnO_2

System	σ $(\Omega\ cm)^{-1}$
Pure SnO_2	0.16
Mo-doped SnO_2	2.84×10^2
Nb-doped SnO_2	3.61×10^3
Ta-doped SnO_2	8.48×10^3

electronic configuration between native and dopant elements. In addition, both Nb- and Ta-dopant improve the electrical conductivity more quantitatively than that of Mo-dopant. These could be contribute to shallow donor states created by Nb- and Ta-dopant close to the conduction band; therefore, the electrons could be excited by low energy.

4 Conclusion

We have investigated the structural, electronic, optical and electrical properties of pure-, Mo-, Nb- and Ta-doped SnO_2. We first study the effect of dopant on the thermodynamic stability of rutile-SnO_2 by calculating the formation energies and reveal that the doped systems remain stable after doping. The optical response shows the red-shifting of the transmittance curve in the case of Mo- and Nb-doped SnO_2 due to reduce in the band gap, whereas, show the blue-shifting in the case of Ta-doped SnO_2 owing to expand in the optical band gap according to the Burstein-Moss effect. The semiclassical Boltzmann transport calculations demonstrate that the electrical conductivity is significantly enhanced for doped SnO_2, with the highest increasing in the case Ta-doped SnO_2 system. Finally, our results reveal that the Ta-doped SnO_2 could be useful as a transparent conducting oxide.

References

Amin, B., Ahmad, I., Maqbool, M., Goumri-Said, S., Ahmad, R.: Ab initio study of the bandgap engineering of $Al_{1-x}Ga_xNAl_{1-x}Ga_xN$ for optoelectronic applications. J. Appl. Phys. **109**, 023109 (2011)

Bai, J., Raulot, J.M., Zhang, Y.D., Esling, C., Zhao, X., Zuo, L.: Crystallographic, magnetic, and electronic structures of ferromagnetic shape memory alloys Ni2XGa (X = Mn, Fe, Co) from first-principles calculations. J. Appl. Phys. **109**, 014908 (2011)

Blaha, P., Schwarz, K., Madsen, G.K.H., Kvasnicka, D., Luitz, J.: In: Schwarz, K. (ed.) WIEN2K: An Augmented Plane Wave and Local Orbitals Program for Calculating Crystal Properties. Vienna University of Technology, Austria (2001)

Dixit, H., Saniz, R., Cottenier, S., Lamoen, D., Partoens, B.: Electronic structure of transparent oxides with the Tran–Blaha modified Becke–Johnson potential. J. Phys. Condens. Matter **24**, 205503 (2012)

Duan, Y.H.: Electronic properties and stabilities of bulk and low-index surfaces of SnO in comparison with SnO_2: a first-principles density functional approach with an empirical correction of van der Waals interactions. Phys. Rev. B **77**, 045332 (2008)

Gao, Q., Li, M., Liu, Q., Wang, Y., Li, X., Wei, X., Song, C., Wang, J., Liu, J., Shen, G., Han, G.: Enhanced preferential orientation and electrical property of fluorine-doped SnO_2 thin films via barrier layer. Mater. Lett. **122**, 143–146 (2014)

Hassan, F.E.H., Alaeddine, A., Zoaeter, M., Rachidi, I.: First-principles investigation of SnO_2 at high pressure. Int. J. Mod. Phys. B **19**, 4081–4092 (2005)

Kim, G.K.H., Lee, S.W., Shin, D.W., Park, C.G.: Effect of antimony addition on electrical and optical properties of tin oxide film. J. Am. Ceram. Soc. **77**, 915–921 (1994)

Madsen, G.K.H., Blaha, P., Schwarz, K., Sjöstedt, E., Nordström, L.: Efficient linearization of the augmented plane-wave method. Phys. Rev. B **64**, 195134 (2001)

Madsena, G.K.H., Singh, D.J.: BoltzTraP. A code for calculating band-structure dependent quantities. Comput. Phys. Commun. **175**, 67–71 (2006)
Murnaghan, F.D.: The compressibility of media under extreme pressures. Proc. Natl. Acad. Sci. USA **30**, 244–247 (1944)
Okoye, C.M.I.: Theoretical study of the electronic structure, chemical bonding and optical properties of KNbO3 in the paraelectric cubic phase. J. Phys. Condens. Matter **15**, 5945–5958 (2003)
Ong, K.P., Singh, D.J., Wu, P.: Analysis of the thermoelectric properties of n-type ZnO. Phys. Rev B **83**, 115110 (2011)
Orel, B., Lavrenčič Štangar, U., Opar, U., Gaberšček, M., Kalche, K.: Preparation and characterization of Mo- and Sb: Mo-doped SnO_2 sol–gel-derived films for counter-electrode applications in electrochromic devices. J. Mater. Chem. **5**, 617–624 (1995)
Ouerfelli, J., Djobo, S.O., Bernède, J.C., Cattin, L., Morsli, M., Berredjem, Y.: Organic light emitting diodes using fluorine doped tin oxide thin films, deposited by chemical spray pyrolysis, as anode. Mater. Chem. Phys. **112**, 198–201 (2008)
Park, J.Y., Zhao, X.G., Gu, H.B.: Synthesis and characterization of SnO_2 nanostructure using *Bombyx mori* (L.) silkworm cocoon as biomass template for photocatalytic reaction. Mater. Lett. **141**, 187–190 (2015)
Perdew, J.P., Burke, K., Ernzerhof, M.: Generalized gradient approximation made simple. Phys. Rev. Lett. **77**, 3865–3868 (1996)
Qin, G., Li, D., Feng, Z., Liu, S.: First principles study on the properties of p-type conducting In: SnO_2. Thin Solid Films **517**, 3345–3349 (2009)
Scheidemantel, T.J., Ambrosch-Draxl, C., Thonhauser, T., Badding, J.V., Sofo, J.O.: Transport coefficients from first-principles calculations. Phys. Rev. B **68**, 125210 (2003)
Shi, L.-B., Dong, H.-K., Qi, G.-Q.: Density functional theory description of origin of ferromagnetism in Cu doped SnO_2. J. Magn. Magn. Mater. **345**, 215–221 (2013)
Singh, A.K., Janoti, A., Scheffler, M., Van de Walle, C.G.: Sources of electrical conductivity in SnO_2. Phys. Rev. Lett. **101**, 055502 (2008)
Singh, R., Kumar, M., Shankar, S., Singh, R., Ghosh, A.K., Thakur, O.P., Das, B.: Effects of Sb, Zn doping on structural, electrical and optical properties of SnO_2 thin films. Mater. Sci. Semicond. Process. **31**, 310–314 (2015)
Slassi, A.: Ab initio study of a cubic perovskite: structural, electronic, optical and electrical properties of native, lanthanum- and antimony-doped barium tin oxide. Mater. Sci. Semicond. Process. **32**, 100–106 (2015)
Slassi, A., Naji, S., Benyoussef, A., Hamedoun, M., El Kenz, A.: On the transparent conducting oxide Al doped ZnO: first principles and Boltzmann equations study. J. Alloys Compd. **605**, 118–123 (2014)
Sun, J., Wang, H.-T., He, J., Tian, Y.: Ab initio investigations of optical properties of the high-pressure phases of ZnO. Phys. Rev. B **71**, 125132 (2005)
Toyosaki, H., Kawasaki, M., Tokura, Y.: Electrical properties of Ta-doped SnO_2 thin films epitaxially grown on TiO_2 substrate. Appl. Phys. Lett. **93**, 132109 (2008)
Tran, F., Blaha, P.: Accurate band gaps of semiconductors and insulators with a semilocal exchange-correlation potential. Phys. Rev. Lett. **102**, 226401 (2009)
Tsubota, T., Kobayashi, S., Murakami, N., Ohno, T.: Improvement of thermoelectric performance for Sb-doped SnO2 ceramics material by addition of Cu as sintering additive. J. Electron. Mater. **43**, 3567–3573 (2014)
Turgut, G., Keskenler, E.F., Aydın, S., Sönmez, E., Doğan, S., Düzgün, B., Ertuğrul, M.: Effect of Nb doping on structural, electrical and optical properties of spray deposited SnO_2 thin films. Superlattices Microstruct. **56**, 107–116 (2013)
Yates, H.M., Evans, P., Sheel, D.W., Nicolay, S., Ding, L., Ballif, C.: The development of high performance SnO2: F as TCOs for thin film silicon solar cells. Surf. Coat. Technol. **213**, 167–174 (2012)
Zhang, G., Qin, G., Yu, G., Hu, Q., Fu, H., Shao, C.: Ab initio investigation on a promising transparent conductive oxide, Nb:SnO_2. Thin Solid Films **520**, 5965–5970 (2012)